Journal Pre-proof



Design and performance of solar concentrator assisted photocatalytic reactors for solar-to-hydrogen conversion

Aman Dhiman, Ehsan Ghanbari Kohyani, Harjit Singh, Nathan Skillen, Virendra Vijay, Ahmed Ghitas

PII: S1385-8947(26)11279-0

DOI: https://doi.org/10.1016/j.cej.2026.183816

Reference: CEJ 183816

To appear in:

Received date: 8 May 2026

Revised date: 11 August 2026

Accepted date: 22 October 2026

Please cite this article as: A. Dhiman, E.G. Kohyani, H. Singh, et al., Design and performance of solar concentrator assisted photocatalytic reactors for solar-to-hydrogen conversion, (2026), https://doi.org/10.1016/j.cej.2026.183816

This is a PDF of an article that has undergone enhancements after acceptance, such as the addition of a cover page and metadata, and formatting for readability. This version will undergo additional copyediting, typesetting and review before it is published in its final form. As such, this version is no longer the Accepted Manuscript, but it is not yet the definitive Version of Record; we are providing this early version to give early visibility of the article. Please note that Elsevier's sharing policy for the Published Journal Article applies to this version, see: https://www.elsevier.com/about/policies-and-standards/sharing#4-published-journal-article. Please also note that, during the production process, errors may be discovered which could affect the content, and all legal disclaimers that apply to the journal pertain.

© 2026 Published by Elsevier B.V.

Journal Pre-proof

Design and performance of solar concentrator assisted photocatalytic reactors for Solar-to-Hydrogen conversion

Aman Dhiman[a], Ehsan Ghanbari Kohyani[a], Harjit Singh[a,*] harjit.singh@brunel.ac.uk, Nathan Skillen[b], Virendra Vijay[c], Ahmed Ghitas[d]

[a]Department of Engineering, Brunel University of London, Uxbridge, UB8 3PH, United Kingdom

[b]International Centre for Brewing and Distilling, School of Engineering and Physical Sciences, Heriot-Watt University, Edinburgh, EH14 4AS, United Kingdom

[c]Centre fort Rural Development and Technology, Indian Institute of Technology Delhi, New Delhi, 110016, India

[d]National Research Institute of Astronomy and Geophysics, Cairo, 11421, Egypt

[*]Corresponding author.

Abstract

Solar-powered water splitting via photocatalysis provides a sustainable method towards low-carbon hydrogen generation. However, efficient capture and utilisation of solar energy remains a key challenge for existing reactor designs. Whilst Compound Parabolic Concentrators (CPCs) can enhance the Solar-To-Hydrogen (STH) efficiency of photocatalytic systems, to date the optimal designs have not been developed. To address this knowledge gap, we report a methodology to design optimised solar photocatalytic reactors and predict their performance for maximum hydrogen production. Reactor design features for four geographically diverse locations – London, Cardiff, Cairo and Chennai – are presented and shown to achieve Annual Optical Efficiency (AOE) of 74.2%, 78.4%, 89.1% and 84.8% respectively. The model incorporates real life solar and climatic conditions with accompanying experiments enabling validation of the model results. Experimental data is used to predict the total hydrogen production for peak summer months for several geometric configurations across all four locations. Experimental results show that STH peaked at 353 K. This integrated experimental-computational framework provides valuable insights into the optimisation of solar concentrator design to maximise hydrogen generation and advances the development of sustainable hydrogen production technologies.

Keywords

Sustainable Hydrogen, Photocatalysis, Compound Parabolic Concentrator, COMSOL Multiphysics, Water splitting, Location specific reactor designs

1. Introduction

Photocatalytic generation of hydrogen, first reported in 1972 [1], has since attracted extensive research efforts focussed on producing photocatalyst materials with better charge separation and enhanced light absorption [2–4]. Despite significant progress in material advancements, a key barrier remains the low Solar-To-Hydrogen (STH) efficiency of the photocatalytic water splitting process, which hinders the economic competitiveness of the technology in comparison to other production methods [5–7]. To date, the highest STH reported under outdoor natural conditions is 9% which was achieved using concentrated solar radiation (Concentration ratio (CR) ~ 190) enabled by a Fresnel lens [8] in conjunction with $Rh/Cr_2O_3/Co_3O_4$ loaded InGaN/GaN nanowired catalyst. Although, the number is impressive, there are challenges associated with scalability due to the use of noble elements rhodium, Indium and Gallium. Additionally, this STH was demonstrated at a small scale, 16

cm^2, which does not guarantee performance at large scale. In contrast, photocatalytic hydrogen production based on a range of more abundant and scalable materials (e.g. oxides, sulphides, oxynitrides) typically report STH lower than 2% under both controlled laboratory [9–12] and outdoor conditions [13–15]. This low STH needs to be balanced with scalability and low-cost materials to make the system economically viable. Increased radiation intensity and elevated operating temperature have been reported to enhance photocatalytic activity for solar hydrogen production but only up to a certain catalyst dependent threshold beyond which performance saturates or declines due to recombination and stability limitations [8,12,16–18]. The technology is still predominantly limited to a low Technology Readiness Level of 2-4, with most studies confined to laboratory scale demonstrations. Current technology status suggests a widening of the gap between fundamental research and real-world deployment which is heavily reflected in the lack of pilot scale studies. If unaddressed, this gap is likely to further widen. A transition from materials science to engineering is needed with greater emphasis placed on the system level challenges such as efficient utilisation of solar energy, scalability of reactors and long-term deployment of reactor systems.

Recently studies have increasingly focussed on the scalability aspect of the technology. Zhao et. al. [19] proposed a hydrogen farm strategy based on modular particulate photocatalyst reactor sheets integrated with centralised electrolyser, demonstrating the potential for large scale deployment at an estimated TRL of 5-6. However, the dependence on electrolysers increases system complexity and capital cost, highlighting the need for independent photocatalytic reactor system. For example, carbon nitride based photocatalyst in a continuous flow photoreactor demonstrated improved photon utilisation and scalability potential, considered approx. TRL 4-5 [20]. Photocatalytic hydrogen generators that can harness wider solar spectrum (UV-Visible-IR) are needed to be demonstrated eventually lead to an economically viable large-scale deployment. For example, a pilot-scale green hydrogen production under concentrated sunlight highlighting the synergistic benefits of photothermal effects and solar concentration for overall water splitting reported by Wang et al [21]. Given the reported pilot scale, outdoor, integrated demonstration, this work can be addressed as TRL 7. Scaling efforts could be as well accelerated by learning from cross-disciplinary studies such as production of hydrogen peroxide using $1m^2$ photocatalytic flow reactor (TRL 6-7) [22].

Solar concentrators have been investigated to enhance photon flux and exploit thermal effects for enhanced hydrogen production [23]. Recently, Avargani et al. [24] reported a validated CFD modelling based study for the integration of solar concentrators with photoreactors. Wang et al. [25] developed a linear elliptical shaped concentrator integrated with a tubular photoreactor and examined the effects of concentrated light intensity and thermal energy on the hydrogen production performance. Ma et al. [26] studied the use of optical concentrators for simultaneous production of hydrogen and electricity. Holmes-Gentle et al. [27] proposed a kilowatt scale solar hydrogen system using concentrated light. While these studies provide a strong basis for the development of solar integrated reactor systems, there are associated limitations with each of them. For example, Parabolic dish collectors [24,27] need dual axis tracking and precise alignment, linear elliptical concentrators [25] and Fresnel lenses [8,26] suffer from issues like optical complexity, overheating and require a sun tracker.

In this context, Compound Parabolic Concentrators (CPCs), due to a wide acceptance angle

and ability to harness a significant proportion of diffused sunlight without requiring complex sun-tracking [28,29] are considered a strong candidate. CPCs have been extensively investigated for their use in solar thermal and photovoltaic systems [30–32], however a very limited number of studies have reported their utilization for photocatalytic hydrogen production. Some exceptions are Jing et al. [33] and Wei et al. [34], with the later reporting a solar field comprising 76 CPC units with a light accepting area of 103.7 m^2. It was further demonstrated that a Surface Uniform Concentrator (SUC), developed through modifications to an existing CPC design, can enhance the STH by 8.57% under the same weather and solar considerations [35–37]. A subsequent pilot scale study highlighted the importance of local weather and solar trajectories in selecting an appropriate CR but does not report the effect of these conditions on the annual optical efficiency and hydrogen production [38,39]. SUCs [36] require constant solar tracking to focus the concentrated radiation over the reactor tube. Despite these efforts, an optimal design for the CPC collectors have not been developed yet. It is well known that concentrator geometry plays a critical role in achieving high optical efficiencies of solar radiation on the reactor surface and that this relationship is strongly influenced by local meteorological conditions and solar trajectories. Current design methodologies, however, do not explicitly integrate these location specific factors into the optimisation process for photocatalytic hydrogen reactors [40,41]. Furthermore, there are no studies which have predicted the annual optical and thermal performance of CPC based photocatalytic hydrogen production systems under realistic, time resolved outdoor conditions. Such studies should incorporate solar positions algorithms, variations in irradiance and system level factors such as reactor orientation and seasonal adjustments. This is a crucial consideration as CPC geometry for a specific location might not be suitable for other locations. Regions which receive more direct light may favour a low CR to maintain a prescribed temperature range, while a location like London, with around 55% average annual diffuse radiation, may require a high CR to achieve the required thermal conditions. This spatial variability defines the need for a location specific optimisation framework.

To address these critical gaps, this paper reports a validated methodology for designing location-specific optimal photocatalytic hydrogen reactors integrated with CPC reflectors (Fig. 1). A ray heating module in COMSOL Multiphysics was used to perform detailed optical and thermal simulations. Four geographically diverse locations - London, Cardiff, Cairo and Chennai - were selected to demonstrate the application. These locations were chosen to capture diverse climatic conditions and solar trajectories. Rather than exploring an extensive range of catalysts, the study focusses on TiO_2, which is widely used in photocatalysis due to its chemical and thermal stability, corrosion resistivity, off the shelf availability and photocatalytic performance which makes it a suitable candidate for the long term, large scale photocatalytic hydrogen production under natural sunlight [42–44]. The research emphasises the optimisation of reactor geometry tailored to each location to maximise the hydrogen production via maximising annual optical efficiency whilst maintaining the optimal reactor temperature without sun-tracking. Extensive indoor experiments were conducted under simulated and artificial radiation sources with the measured data used to predict hydrogen production at various CRs across all four locations. The optimal reactor orientation was determined for each site by accounting for the local solar trajectory, ensuring maximum solar collection over the reaction site throughout

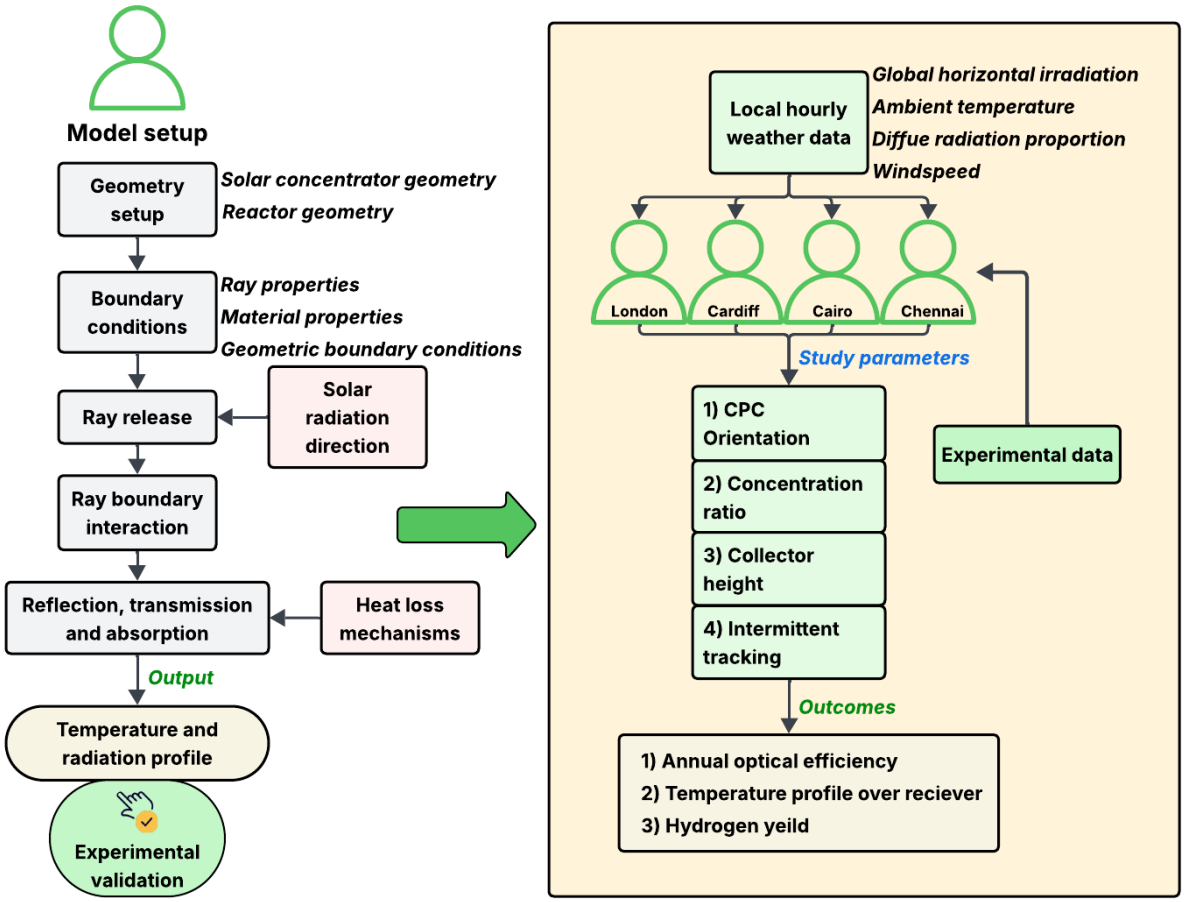


Fig. 1. Flowchart to simulate the temperature profile and solar radiation over reactor and involved study parameters and outcomes.

the year. The findings of this research provide a comprehensive framework for the location-specific photocatalytic hydrogen production reactors, offering valuable insights into how geographical and environmental factors influence the design, orientation and feasibility of such systems.

2. Concentrator geometry and model description

A flat plate reactor integrated with immobilised photocatalyst, TiO_2-P25, illuminated by radiation coming after reflection from CPC reflectors was modelled in COMSOL Multiphysics environment considering the long-term utilisation view, less complexity and easy scalability of the reactor system. Immobilised photocatalyst on a solid substrate provides several advantages over suspended systems including better charge separation, lower or nil loss of photocatalyst material, improved durability and scalability [15,18,45,46]. Additionally, this configuration provides better precise control over catalyst distribution, enabling better light absorption and energy conversion. A flat panel stainless-steel reactor measuring 133.2mm × 1800mm × 2.5mm supporting a 6.8 mm thick water layer, as shown in Fig. 2, was modelled. Acrylic plate with high transmittance (80-90%) in the UV-A region, which is the overlapping spectrum for TiO_2 absorption [47], was used as top cover for water channel. The CPC geometry was generated using the equations (1) and (2).

$$x = d\,\frac{(1+sin\theta)\cdot sin\emptyset}{1-cos(\theta+\emptyset)} - \frac{d}{2} \quad (1)$$

$$y = d\,\frac{(1+sin\theta)\cdot cos\emptyset}{1-cos(\theta\ +\emptyset)} \qquad (2)$$

where x and y are the coordinates of the parametric curve for CPC geometry, d the reactor width, θ the half acceptance angle and $\emptyset$, the variable angle parameter. In equations (1) and (2), the angular limits are described by

$$\theta < \emptyset < \frac{\pi}{2}$$

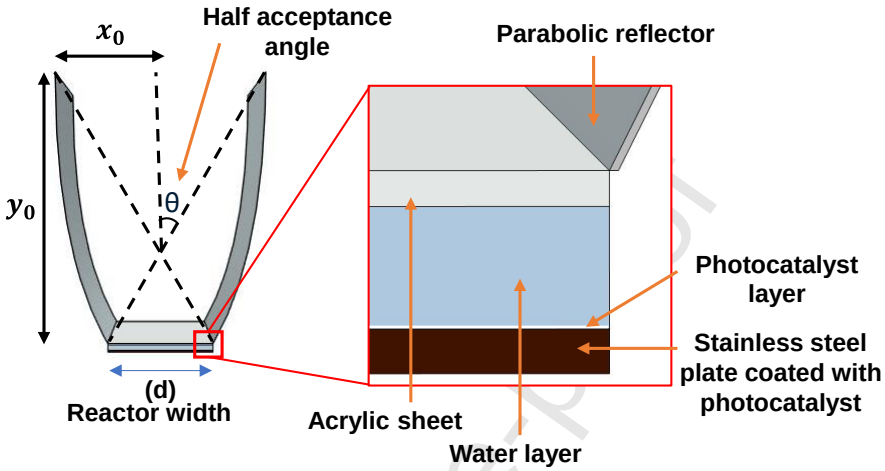


Fig. 2. CPC reflector with flat reactor modelled (not to scale)

The reactor width was fixed at 133.2 mm whilst CR and height of concentrators was varied to find the best geometry suitable for each location. For CPCs, aperture to height ratio decreases with increasing CR, Electronic Supplementary Information (ESI) Fig. S1 (blue curve) and ESI S2 (a-e), so concentrators with high CR are not easy to manufacture. Regulating height using conventional truncation won't help in achieving the desired height and CR at the same time as only one parameter can be fixed, and other will come as an output. Conventionally, θ is specified, and $\emptyset$ swept across the parametric equation (1) and (2) to get the final profiles of the parabolic sides of a CPC.

In this study, we are using an inverse approach in which desired half aperture width (x_0) and full height (y_0) were used as input parameters. The output was achieved by solving the equations (1) and (2) to determine the pair $(\theta, \emptyset_{min})$ that would determine the curve satisfying, $x(\emptyset_{min}) = x_0$ and $y(\emptyset_{min}) = y_0$, where $\emptyset_{min}$ is the lower limit of variable angle parameter at point (x_0, y_0) on the curve. The pair $(\theta, \emptyset_{min})$ was calculated for different combinations of reflector height and CR used in this study as shown in ESI Table S1. CR was varied from 1.75 to 3.5 and height was varied from 200 mm to 346.1 mm except for the CPC with CR 1.75 for which height was varied from 100 mm to 250 mm. This was done because 250 mm is the full height for a concentrator with a CR of 1.75 and it's not practically beneficial to design CPC concentrators higher than the geometric full height. The same approach was applied for CR 1.5 for which a full height of 186.2 mm was used. Our approach can effectively invert the CPC design process by providing a direct pathway for customized CPC geometry, se ESI Fig. S1 (orange line) and ESI Fig. S2 (f-j). Detailed model description and applied boundary conditions is provided in ESI section S1. A mesh convergence study was performed to assess the effect of mesh density on the simulation results and to identify

the optimal mesh size and optimal number of incident rays as explained in ESI section S1.3 and ESI Fig. S5. “Fine” mesh size and 7000 incident rays was adopted for simulations. Experimental validation was carried out by using a geometrically scaled reactor with same material properties, heat transfer characteristics and boundary conditions, which are scale independent. Mesh-independent solutions were obtained for the small reactor as well, see ESI section S1.3 and ESI Fig. S6, and the validated numerical framework subsequently employed to predict thermal and optical behaviour of a large-scale reactor under solar concentration.

Experimental validation

Experimental validation of the numerical model was performed using a flat panel reactor (stainless steel, 150mm × 50mm × 1mm, water layer thickness 6mm) integrated with a CPC reflector (CR 3, height 135 mm, aperture width 150 mm) as shown in ESI Fig. S5b. The stainless-steel plate was coated with photocatalyst (TiO_2) employing a spray coating technique, which is detailed in ESI section S2**.** Experiments were performed under a solar simulator (OAI Trisol, Model TSS - 156) with AM 1.5G filter with an illuminated area of 150mm × 150mm as shown in Fig. 3a. Five K-type calibrated thermocouples (error ±0.6%) were deployed to measure reactor temperature. A maximum temperature of 343.8 K was recorded at the mid-point of the reactor plate; temperature deceased gradually towards the edges; see Fig. 3c and 3d. This trend is due to more concentrated radiation within the middle part when incident rays are normal to the reactor plate (Fig. 3b). A strong correlation between measured and simulated results was found with a standard deviation of 2.77 and R^2 value of 0.86. The experimentally measured temperatures represent steady state condition, which include heat build-up over time. Consequently, the experimental temperature values are more uniformly distributed across the reactor. The simulated and experimental temperatures showed a good agreement in the whole, validating the reliability and accuracy of the computer model developed.

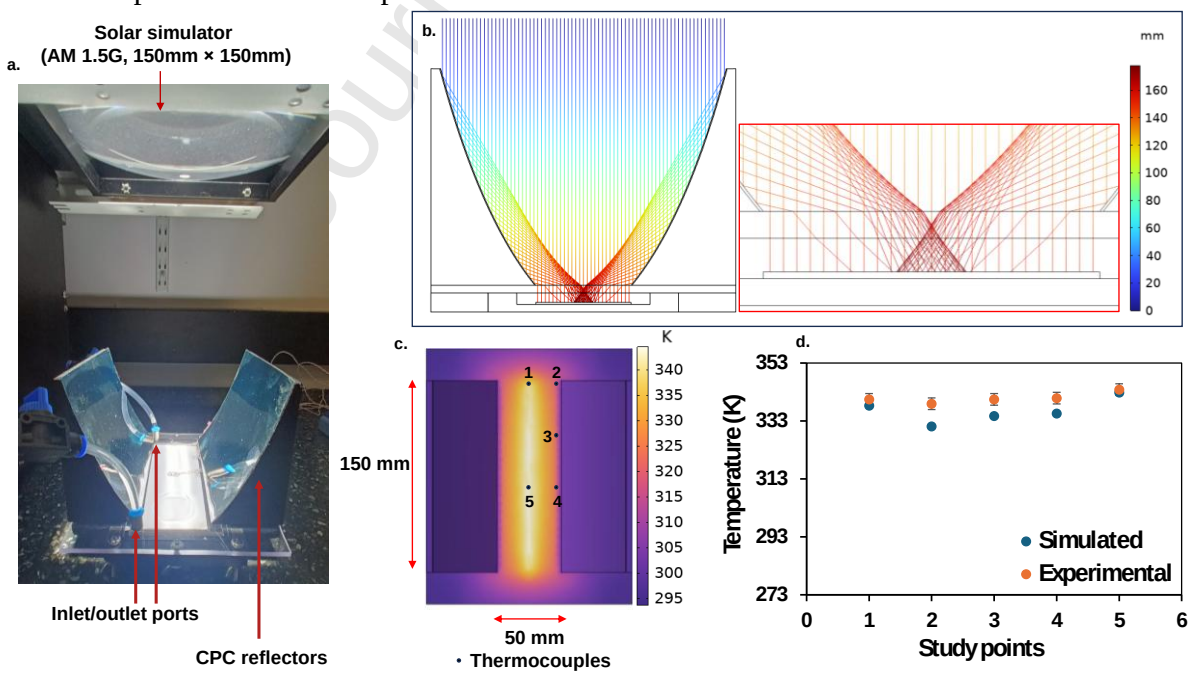


Fig. 3. a. Experiments conducted under solar simulator equipped with AM 1.5G filter for validating the computer model developed, **b.** Concentrated radiation profile over the reactor

plate (legend: ray optical path length), **c.** Temperature profile generated and **d.** simulated and experimental results comparison.

3. Results and discussion

The geometry of the CPCs was iteratively optimised to maximise the hydrogen production for peak solar months. Hydrogen production is governed by both the STH efficiency and incident solar irradiance over reactor plate, while STH itself is strongly dependent on the operating temperature of the system. Experiments were conducted to evaluate the dependency of STH efficiency over the operating temperature (Section 3.1). The CPC orientation was optimised for each location to maximise the AOE at different tilt angles (Section 3.2). Using the experimental data from section 3.1 together with the generated temperature profile and corresponding solar radiation, hydrogen production rate was estimated at optimal orientation and varied CRs for each location (section 3.3). The height of the CPC collectors was optimised at optimal CR and orientation for each location (Section 3.4). Intermittent tracking was proposed for London and Cardiff due to relatively low AOE values, 57.4% and 66.1% respectively, to enhance the performance in these locations (Section 3.5).

3.1 Hydrogen production experiments

Hydrogen experiments were carried out, by using the same reactor that was employed for validation, under polychromatic light source (300 W, high pressure mercury lamp (280 nm – 2000 nm)). The purpose was to evaluate the effect of reaction temperature over the hydrogen production rate. The experimental setup is shown in Fig. 4a and 4b. Materials and apparatus used are provided in ESI section S3. Pristine TiO_2-P25 was used as a benchmark photocatalyst without the use of any cocatalysts. The optical properties of the photocatalyst were characterised by using UV-vis spectroscopy as shown in ESI Fig. S7a, revealing a band gap of 3.22 eV. XRD analysis showed the presence of both anatase and rutile phases with high crystallinity, see ESI Fig. S7c.The photocatalyst coating, composed of TiO_2-P25 nanoparticles (particle size ~ 20-25 nm, see Fig. ESI S7b), was deposited on a stainless-steel plate. Cross sectional analysis revealed a coating thickness of 4-7 μm as shown in ESI Fig. S8. Coating method and characterisation are provided in ESI section S3 and section S4. The coated plate was

Journal Pre-proof

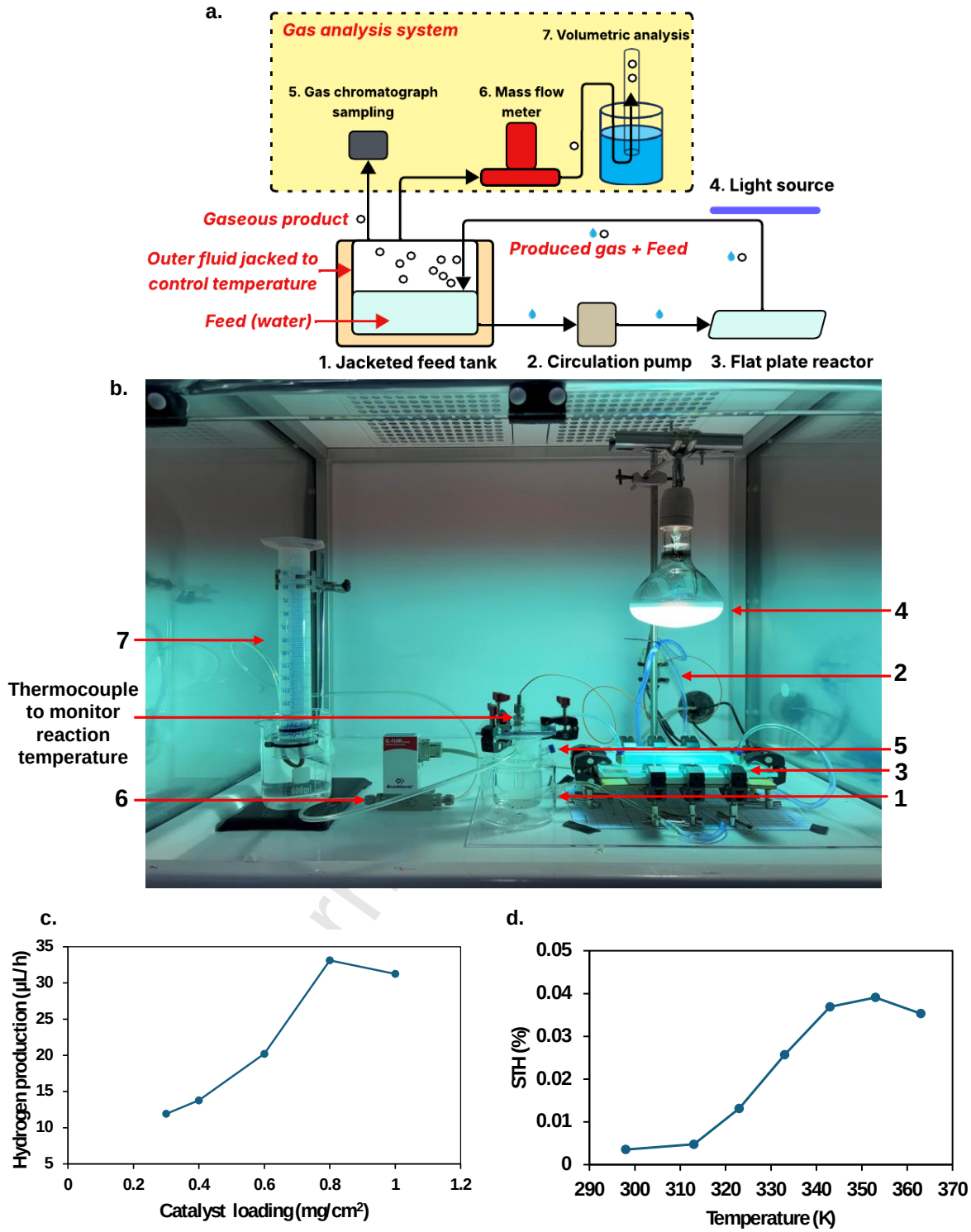


Fig. 4 a. Schematic of experimental setup**, b.** Experimental setup, **c.** Hydrogen production at different catalyst loading at 323 K and **d.** STH efficiency at different operating temperatures at 0.8 mg/cm^2 catalyst loading. *Catalyst coated area = 75 cm^2*

mounted on an outer frame and sealed with an acrylic cover using silicon O-ring and clamps. Distilled water was used as feedstock and circulated through a jacketed feed tank at a flow rate of 0.4 L/min using a circulation pump. No sacrificial agents were utilised in the reaction. Before initiating the reaction, the reaction chamber, including the reactor, feed tank and

polyurethane tubes, was purged with nitrogen for 20 minutes to remove residual air and ensure an inert environment. The gaseous product produced in the reactor travelled with circulated water and accumulated in the head space of the feed tank as shown in Fig 4a. The system comprised a total working volume of 279 mL (reactor, feed tank and connecting polyurethane tubes) of which 229 mL was filled with water, leaving a fixed headspace of 50 mL in the feed tank. The collected gases were withdrawn from the top outlet of the feed tank using a gas tight syringe and analysed using a gas chromatograph (Agilent 7280A, thermal conductivity detector, Ar carrier gas, packed column (RESTEK)) Reaction temperature was controlled by circulating heated water in the outer jacket of the feed tank and was continuously monitored and adjusted to maintain the desired reactor conditions. 5 samples with different catalyst loading from 0.3 to 1 mg/cm^2 were tested. The results showed that 0.8 mg/cm^2 provided optimal performance after which activity doesn't improve further for water splitting reaction as shown in Fig. 4c. The optimal loading sample then used for temperature dependent study and findings showed that STH efficiency increased with temperature peaking at 353 K as shown in Fig. 4d. An optimal range was chosen out to be 353 ± 10 K as the deviation is less than 10% from the maximum value in this range. Although, the experimental results identified the optimal operating temperature for achieving maximum STH efficiency, maintaining which under natural outdoor conditions through the year will be challenging due to dynamic solar and weather conditions. Therefore, CPC orientation and geometry is optimised in the next sections to maximise the number of hours in the optimal temperature range.

3.2. Solar Collector orientation

The orientation of solar concentrators significantly impacts their optical efficiency, which is vital for hydrogen production, and fixed non-tracking solar collectors must sacrifice some optical performance due to continually changing solar trajectory throughout the day. Sun apparently sweeps through an angular expanse of 15°/hour in the sky from east to west. For north-south placement of CPC, it would require a half acceptance angle of greater than 60° considering fixed orientation for minimum 8 hours of daily operation. This will be too large of a half acceptance angle for a CPC to concentrate effectively. Therefore, east-west orientation was selected. Concentrators orientated in true south direction (collector azimuth of 0°) were tested to determine the tilt angle that provided the maximum annual solar irradiation on the reactor. For each location, the hourly concentrated solar radiation received over the reactor surface at different tilt angles, from sunrise to sunset were predicted for the whole year considering continuously changing annual solar trajectory. AOE was calculated

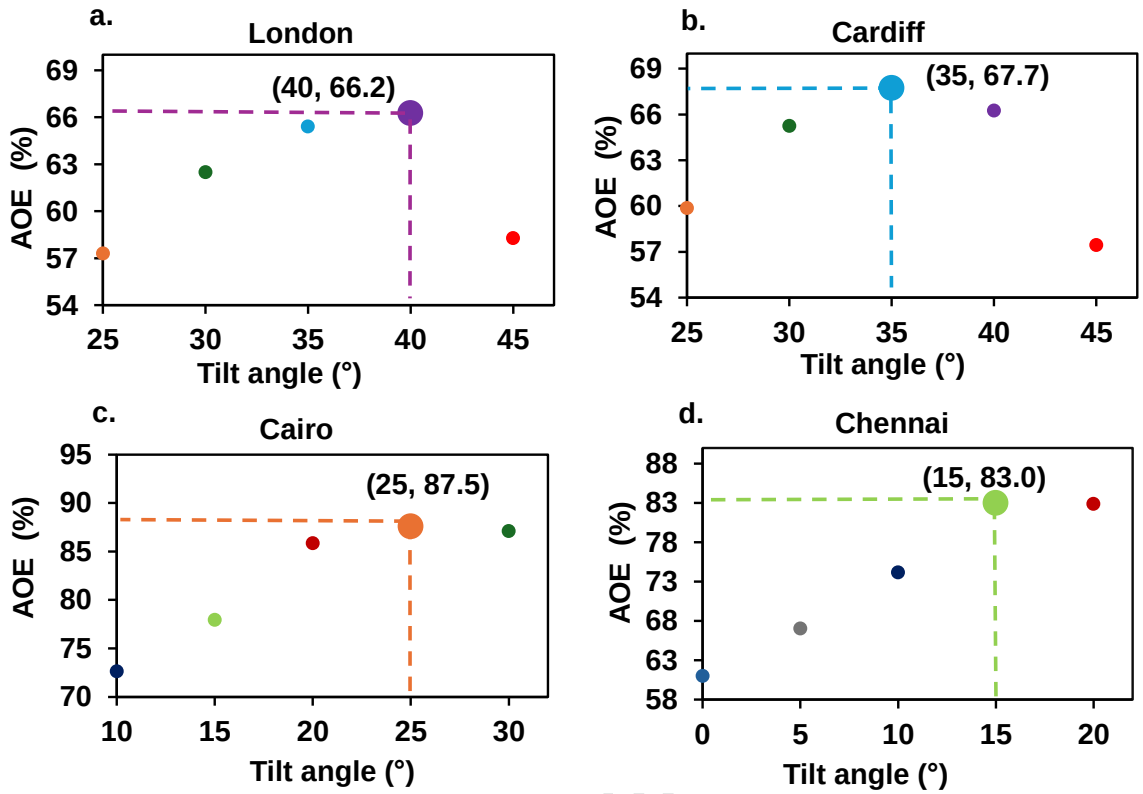


Fig. 5. AOE achieved at different tilt angles for corresponding starting CR for a daily operation from sunrise to sunset over the year for **a.** London, **b.** Cardiff, **c.** Cairo and **d.** Chennai.

considering only the direct radiation, since the objective of the analysis was to optimise CPC orientation on which non-directional diffuse radiation has no influence. Optical losses at reflector and acrylic surfaces and inside water layer were accounted for. Tilt angle optimisation is independent of the CR, therefore at this stage, a representative CR was assumed (CR 3 for London and Cardiff and CR 2 for Cairo and Chennai), only as a geometric reference and does not influence the outcome of the orientation optimisation. All the simulations performed in this section is at same CPC height, 346.1 mm, see ESI Fig. 2. Reflectance, absorbance and transmittance were considered for the materials involved in the ray path. The tilt angle range was selected keeping in view the geographical latitude of a given location; for near-equator regions (Chennai, Cairo), lower tilt angles were beneficial due to high solar elevation angle and for higher latitudes (London, Cardiff), steeper tilts were favoured as the solar elevation angle is quite low. For London and Cardiff, the trend of monthly solar radiation achieved over the reactor appeared similar, with Cardiff receiving higher solar irradiation annually, see ESI Fig. S9. The optimum tilt angles for fixed CPC reflectors for maximum AOE were found to be 40°, 35°, 25°, 15° respectively for London, Cardiff, Cairo and Chennai. The maximum AOE for these locations were predicted to be 66.2%, 67.7% 87.5% and 83.0% respectively as shown in Fig. 5. It should be noted that these values do not represent the final AOE as the system geometry has not been optimised yet and they are subject to change with CR and concentrator height. Detailed information for captured solar radiation on reactor site with changing tilt angle is available in ESI Fig. S9. The optimal tilt angles are further used to optimise the CR for each location studied.

3.3. Reactor Temperature profile

Whilst an optimum CPC orientation is important to capture solar radiation efficiently, it does not indicate whether the solar radiation input is sufficient to maintain the reactor within the optimum operating temperature. Moreover, a collector geometry suitable for one location may not achieve same performance elsewhere due to varying solar and weather conditions. Therefore, the optimal orientation determined in section 3.2 along with the local weather data, provided in ESI section S5, were used as an input in the model to generate hourly temperature profile and incident solar radiation over the reactor site from sunrise to sunset daily at various CRs governed by local hourly solar trajectories. Five peak solar radiation months were selected for each location for analysis. April to August for London, Cardiff and Cairo, and February to June for Chennai. The total working hours over these months were distributed across different temperature range, summarised in Fig. 6, to determine total duration within the optimal operating temperature range (353 ± 10 K) at each CR for every location. Using experimental data from section 3.1, hourly STH efficiencies were calculated from the predicted temperature profiles. Hydrogen production for each configuration was subsequently determined using the calculated STH efficiencies and the corresponding incident solar radiation at the receiver as shown in Fig. 7.

Hydrogen production performance was evaluated as both per unit receiver area (red curves, Fig. 7) as well as average STH (green curves, Fig. 7) to determine best CR based on effective solar energy utilisation. Total hydrogen production per unit receiver area increases with CR for all location except for Cairo, where CR 1.75 yields significantly higher hydrogen production as compared to CR 2 and CR 2.5, as shown in Fig. 7 (red curves). This trend for Cairo is due to a higher number of hours within the optimal temperature range at lower CRs as shown in Fig. 6c. It should be noted

Journal Pre-proof

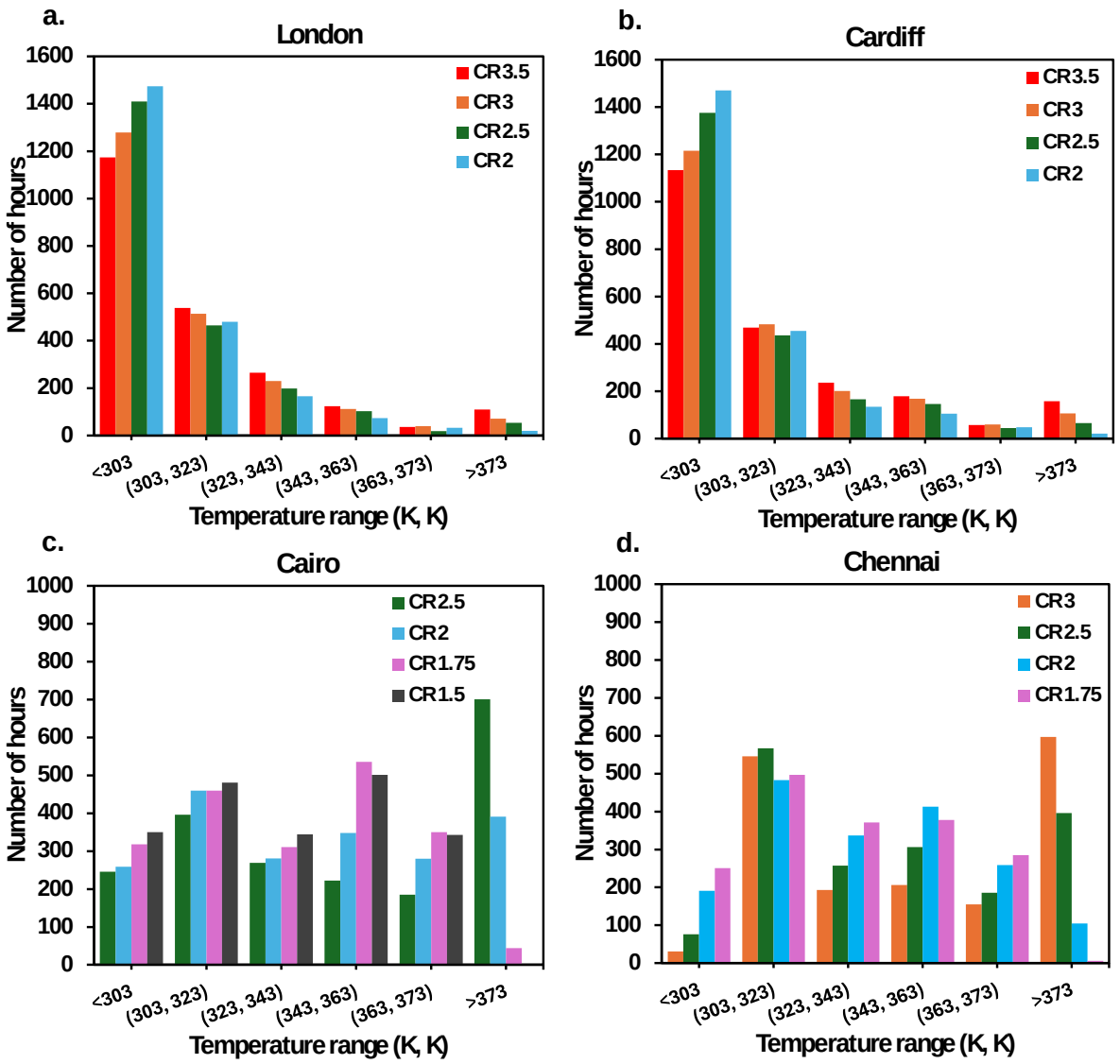


Fig. 6. Hourly temperature profiles at reactor plate for five peak summer months for **a.** London, **b.** Cardiff, **c.** Cairo and **d.** Chennai at different CRs.

that the maximum hydrogen production per unit receiver area does not correspond to optimal system performance. The average STH efficiency, which accounts for the conversion of incident solar energy into chemical energy, provides a more representative metric for overall system performance. STH reveals an optimal CR 3 for both London and Cardiff. Although the duration for London and Cardiff within the optimal temperature range is more for CR 3.5 as compared to CR 3, Fig. 6a and Fig. 6b, the overall solar utilisation efficiency is maximum for CR 3 as shown in Fig. 7a and Fig. 7b (green curves). This is due to the high variation in solar elevation angle at UK

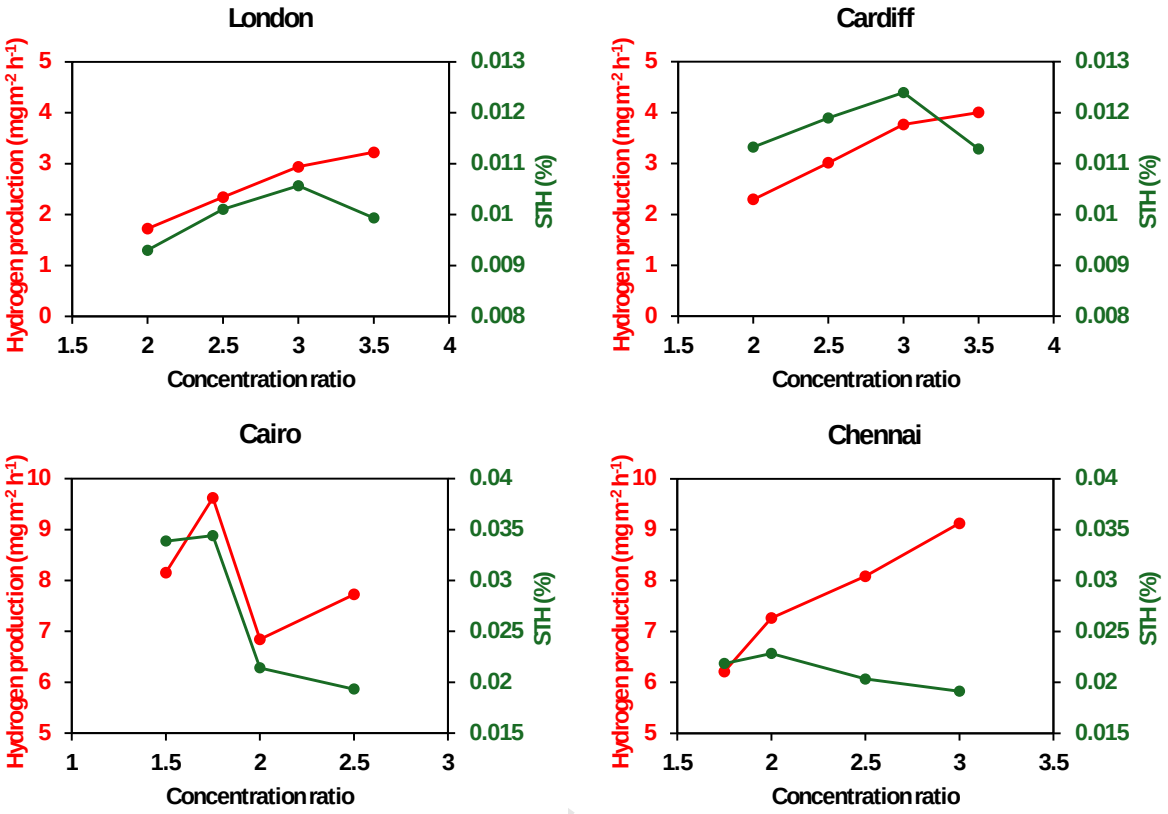


Fig. 7. Average hydrogen production rate per reactor area (red curves) and corresponding STH efficiencies (green curves) for five peak solar months at various CRs for **a.** London, **b.** Cardiff, **c.** Cairo and **d.** Chennai.

locations over these months, which makes it less efficient to harness solar radiation for a collector with high CR. In contrast, Cairo and Chennai achieve optimal performance at lower CRs of CR 1.75 and 2, respectively. It maximises both the duration of operation in optimal working hours, Fig. 6c and Fig. 6d, and hydrogen production relative to solar energy incident over aperture, Fig. 7c and Fig. 7d (green curves). At optimal CR, an average STH of 0.011 %, 0.012 %, 0.034 % and 0.023 % were calculated for London, Cardiff, Cairo and Chennai for five peak solar months.

3.4. Height of CPCs

Truncation is commonly used in CPCs to mitigate the disadvantages like high material cost, inter-row shading, high thermal losses and manufacturing difficulty obtained from a relatively taller CPC. However, truncation is more random than systematic as reducing the collector height while maintaining the desired CR and optical performance is non-trivial. In this section, height of the CPCs was optimised to maximise AOE based on direct beam radiation at optimal orientation and CR, determined in section 3.2 and 3.3 respectively, for each location. The AOE-collector height curve showed distinct trends depending on the geographical location. For UK locations, the AOE reduced with decreasing collector height, see Fig. 8a and Fig. 8b, which is due to the reduction in half acceptance angle which reduces with collector height, see ESI Table S1. However, the reduction in AOE became progressively larger with further decrease in height. Since the objective of truncation is to minimise collector height while maintaining high optical performance, the optimum height was selected at the knee point of the AOE-collector height curve

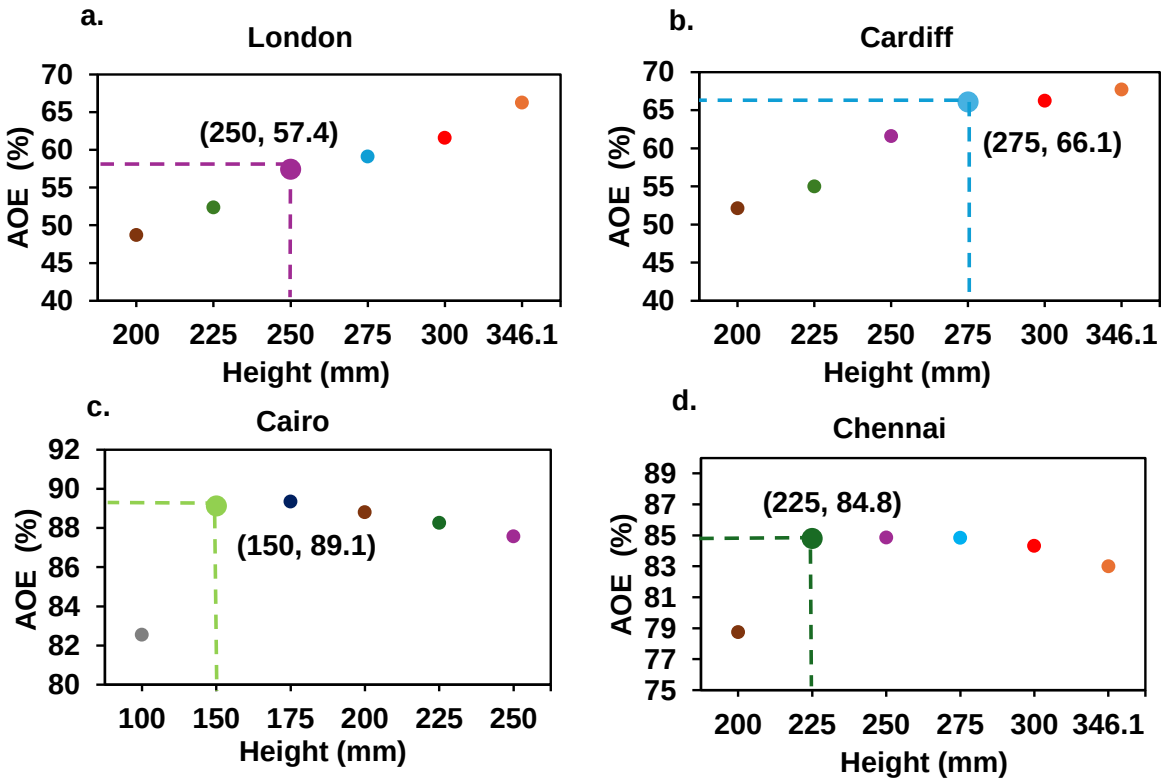


Fig. 8. AOE achieved at different CPC heights for corresponding optimum CR and tilt angle for a daily operation from sunrise to sunset over the year for **a.** London, **b.** Cardiff, **c.** Cairo and **d.** Chennai

after which further reduction in height results in substantially greater loss in AOE for only a small reduction in collector height as shown in Fig. 8a and 8b and ESI Fig. S12. This behaviour indicates that below the knee point, the reduction in collector height increasingly compromises the overall performance of the solar collectors to effectively intercept and concentrate the incident solar radiation towards the reactor aperture as shown in ESI Fig. S12. Based on this criterion, collector height of 250 mm and 275 mm is chosen for London and Cardiff respectively. For Cairo and Chennai, slope for AOE-collector height curve was initially negative with reducing collector height and the height at which the slope transitioned from negative to positive was chosen as the most optimal, as shown in Fig. 8c. and 8d. The corresponding optimum collector heights were 150 mm and 225 mm for Cairo and Chennai respectively. Detailed information for captured solar radiation on reactor with CPC height is provided in ESI Fig. S10. For Cairo and Chennai, the CR is low which on decreasing the height captures solar radiation even more efficiently up to certain height. This is due to high half acceptance angle and less variation in solar elevation angles which does not significantly lowers the annual optical efficiency of the system. In contrast, there was a reduction in AOE for London and Cardiff as the half acceptance angle decreases with decreasing height which makes the system less efficient in capturing solar radiation on annual basis. Therefore, a fixed tilt angle is not recommended for London and Cairo through the year, rather a solar tracking regime should be employed to enhance the AOE as follows in the next section.

3.5. Intermittent tracking system

Best tilt angles for east-west orientated non-tracking CPCs facing true south direction are

detailed in section 3.2. Although the optical performance can be enhanced by introducing sun tracking, the amount of benefit depends strongly on the solar trajectory and CPC geometry at each location. Fig. 8 presents the proportion of solar energy utilized at all four locations at optimal fixed alignment. For Cairo and Chennai, AOE is already quite high (89.1 % and 84.8 % respectively) under fixed installation because the optimum CPC designs employ low CRs of 1.75 and 2 respectively. The low CR corresponds to a larger half acceptance angle, which enables the collectors to accept solar radiation from a wider range of incidence angles without requiring seasonal or monthly realignment. Additionally, the lower latitudes of these two locations result in generally higher solar elevation angle and greater annual solar irradiance. The optimum fixed tilt remains close to the effective solar position for much of the year, leaving small additional radiation to be captured through monthly adjustments. Therefore, sun tracking would not really provide much additional benefit but add complexity to the system at Cairo and Chennai. In contrast, high CR for London and Cardiff provides a comparatively smaller half acceptance angle due to which a fixed tilt is not sufficient to harness solar energy through the year. Furthermore, the higher latitudes and low solar elevation angles of London and Cardiff result in substantial proportion of the annual solar resource occurring during summer months. Consequently, a single fixed tilt angle cannot maintain favourable optical alignment with the solar path resulting in inefficient capture of the solar radiation for the significant portion of the year, particularly during autumn and winter. Therefore, these locations will require the proposed monthly sun-tracking regime. The comparative low AOE values of London (57.4%) and Cardiff (66.1%) can be increased by introducing a less complex monthly sun-tracking (intermittent). The simulations were conducted to identify the best monthly tilt angles to collect the maximum solar radiation for London and Cardiff at optimum values of CR and height. The results are shown in Fig. 9a. and 9b. By introducing monthly tracking, there was an enhancement of 29.1% and 18.7% in the AOE for London and Cardiff respectively giving a final value of 74.2% and 78.4%. The visual representation of captured solar energy on the reactor site for each location is provided in ESI movies M1 and M2.

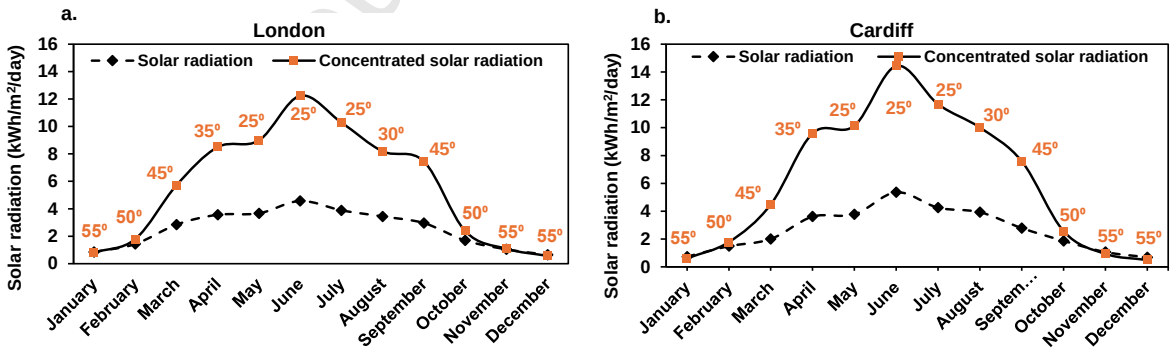


Fig. 9. Monthly solar irradiation harnessed at optimum CR, CPC height and tilt angles for **a.** London and **b.** Cardiff throughout the year

4. Conclusion

A methodology to design concentrating photocatalyst reactors to split water to produce sustainable hydrogen is presented and employed to specify simple, scalable flat panel reactor systems with fixed photocatalyst for four diverse geographical locations – London, Cardiff, Chennai and Cairo. CPC concentrator designs for maximising the amount of solar radiation

reaching the reactor panel are presented as well. Optimum CR, tilt angles, collector height, resulting direct-beam optical efficiencies and hydrogen yield are predicted for all four locations. For example, CRs of 1.75 and 2 and fixed tilt angle of 15° and 25° were found out to be the most optimum for Cairo and Chennai, respectively. A higher CR of 3 was found to be most optimal for London and Cardiff. An intermittent tracking regime was found to yield higher optical efficiency for UK locations. It can be stated that for near equator locations (India, Egypt), CPCs with lower height and CR can provide equivalent photocatalytic reaction conditions to those with higher CR and greater height used in far equator regions (UK). In conclusion, this study provides valuable insights into the optimisation of CPC-integrated photocatalytic hydrogen production systems, demonstrating their potential for efficient and location-specific applications. System scale techno-economic analysis of the solar photocatalytic hydrogen generators is needed to be performed to establish their commercial viability without which bulk uptake will not happen. However, this requires several independent long-term studies to be conducted at different global locations.

Acknowledgement

Authors would like to acknowledge funding received from British Council's ISPF Research Collaboration Programme for PhotoHy project (1203380043), FCDO (UK) for DeSHI project (400020-417) and India's SPARC programme for projects P4053 and P2617. We would like to sincerely thank the Experimental Techniques Centre (ETC) at Brunel for the facilities provided.

Declaration of competing interest

The authors declare that they have no known competing financial interests or personal relationships that could have appeared to influence the work reported in this paper.

References

[1] A. FUJISHIMA, K. HONDA, Electrochemical Photolysis of Water at a Semiconductor Electrode, Nature 238 (1972) 37–38. doi:10.1038/238037a0.

[2] Q. Wang, K. Domen, Particulate Photocatalysts for Light-Driven Water Splitting: Mechanisms, Challenges, and Design Strategies, Chem. Rev. 120 (2020) 919–985. doi:10.1021/acs.chemrev.9b00201.

[3] M. Sohail, S. Rauf, M. Irfan, A. Hayat, M.M. Alghamdi, A.A. El-Zahhar, D. Ghernaout, Y. Al-Hadeethi, W. Lv, Recent developments, advances and strategies in heterogeneous photocatalysts for water splitting, Nanoscale Adv. 6 (2024) 1286–1330. doi:10.1039/d3na00442b.

[4] H. Zhang, J. Liu, T. Xu, W. Ji, X. Zong, Recent Advances on Small Band Gap Semiconductor Materials (≤2.1 eV) for Solar Water Splitting, Catalysts 13 (2023). doi:10.3390/catal13040728.

[5] C. Bie, L. Wang, J. Yu, Challenges for photocatalytic overall water splitting, Chem 8 (2022) 1567–1574. doi:10.1016/j.chempr.2022.04.013.

[6] P. Ravi, J. Noh, Photocatalytic Water Splitting: How Far Away Are We from Being Able to Industrially Produce Solar Hydrogen?, Molecules 27 (2022). doi:10.3390/molecules27217176.

[7] K.H. Ng, S.Y. Lai, C.K. Cheng, Y.W. Cheng, C.C. Chong, Photocatalytic water

splitting for solving energy crisis: Myth, Fact or Busted?, Chemical Engineering Journal 417 (2021). doi:10.1016/j.cej.2021.128847.

[8] P. Zhou, I.A. Navid, Y. Ma, Y. Xiao, P. Wang, Z. Ye, B. Zhou, K. Sun, Z. Mi, Solar-to-hydrogen efficiency of more than 9% in photocatalytic water splitting, Nature 613 (2023) 66–70. doi:10.1038/s41586-022-05399-1.

[9] X. Hao, Y. Shao, D. Xiang, Z. Jin, Photocatalytic overall water splitting hydrogen production over ZnCdS by spatially-separated WP and Co3O4 cocatalysts, Solar Energy Materials and Solar Cells 248 (2022). doi:10.1016/j.solmat.2022.111970.

[10] Q. Wang, T. Hisatomi, Q. Jia, H. Tokudome, M. Zhong, C. Wang, Z. Pan, T. Takata, M. Nakabayashi, N. Shibata, Y. Li, I.D. Sharp, A. Kudo, T. Yamada, K. Domen, Scalable water splitting on particulate photocatalyst sheets with a solar-to-hydrogen energy conversion efficiency exceeding 1%, Nat. Mater. 15 (2016) 611–615. doi:10.1038/nmat4589.

[11] H. Fu, Q. Zhang, Y. Liu, Z. Zheng, H. Cheng, B. Huang, P. Wang, Photocatalytic Overall Water Splitting with a Solar-to-Hydrogen Conversion Efficiency Exceeding 2 % through Halide Perovskite, Angew. Chem. Int. Ed. 63 (2024). doi:10.1002/anie.202411016.

[12] Y. Li, Y.K. Peng, L. Hu, J. Zheng, D. Prabhakaran, S. Wu, T.J. Puchtler, M. Li, K.Y. Wong, R.A. Taylor, S.C.E. Tsang, Photocatalytic water splitting by N-TiO2 on MgO (111) with exceptional quantum efficiencies at elevated temperatures, Nat. Commun. 10 (2019). doi:10.1038/s41467-019-12385-1.

[13] H. Nishiyama, T. Yamada, M. Nakabayashi, Y. Maehara, M. Yamaguchi, Y. Kuromiya, Y. Nagatsuma, H. Tokudome, S. Akiyama, T. Watanabe, R. Narushima, S. Okunaka, N. Shibata, T. Takata, T. Hisatomi, K. Domen, Photocatalytic solar hydrogen production from water on a 100-m2 scale, Nature 598 (2021) 304–307. doi:10.1038/s41586-021-03907-3.

[14] Y. Goto, T. Hisatomi, Q. Wang, T. Higashi, K. Ishikiriyama, T. Maeda, Y. Sakata, S. Okunaka, H. Tokudome, M. Katayama, S. Akiyama, H. Nishiyama, Y. Inoue, T. Takewaki, T. Setoyama, T. Minegishi, T. Takata, T. Yamada, K. Domen, A Particulate Photocatalyst Water-Splitting Panel for Large-Scale Solar Hydrogen Generation, Joule 2 (2018) 509–520. doi:10.1016/j.joule.2017.12.009.

[15] M. Schröder, K. Kailasam, J. Borgmeyer, M. Neumann, A. Thomas, R. Schomäcker, M. Schwarze, Hydrogen Evolution Reaction in a Large-Scale Reactor using a Carbon Nitride Photocatalyst under Natural Sunlight Irradiation, Energy Technology 3 (2015) 1014–1017. doi:10.1002/ente.201500142.

[16] S. Bell, G. Will, J. Bell, Light intensity effects on photocatalytic water splitting with a titania catalyst, Int. J. Hydrogen Energy 38 (2013) 6938–6947. doi:10.1016/j.ijhydene.2013.02.147.

[17] B. Tian, B. Tian, B. Smith, M.C. Scott, R. Hua, Q. Lei, Y. Tian, Supported black phosphorus nanosheets as hydrogen-evolving photocatalyst achieving 5.4% energy conversion efficiency at 353 K, Nat. Commun. 9 (2018). doi:10.1038/s41467-018-03737-4.

[18] C. Pornrungroj, A. Bin Mohamad Annuar, Q. Wang, M. Rahaman, S. Bhattacharjee, V. Andrei, E. Reisner, Hybrid photothermal–photocatalyst sheets for solar-driven overall

Journal Pre-proof

water splitting coupled to water purification, Nature Water 1 (2023) 952–960. doi:10.1038/s44221-023-00139-9.

[19] Y. Zhao, C. Ding, J. Zhu, W. Qin, X. Tao, F. Fan, R. Li, C. Li, A Hydrogen Farm Strategy for Scalable Solar Hydrogen Production with Particulate Photocatalysts, Angew. Chem. Int. Ed. 59 (2020) 9653–9658. doi:10.1002/anie.202001438.

[20] S. Batool, M.Y.S. Ibrahim, F. Ehrlich-Sommer, S.N. Myakala, S. Naghdi, A. Cherevan, Enhanced photocatalytic hydrogen production efficiency using urea-derived carbon nitride in a continuous flow reactor, Sustain. Energy Fuels 9 (2025) 555–564. doi:10.1039/D4SE01239A.

[21] Y. Wang, D. Duan, X. Zhang, Q. Jia, X. Chen, L. Zhong, Y. Li, K. Gan, E. Zhou, Y. Liu, Y. Liu, R. Song, Y. Yang, X. Wu, Pilot-Scale Green Hydrogen Production via Concentrated Natural Sunlight-Driven Photocatalytic Overall Water Splitting and Photothermal Synergy, (2026). doi:10.21203/rs.3.rs-9600220/v1.

[22] X. Zheng, R. Yanagi, Z. Pan, C. Zhou, T. Liu, B. Chen, K. Katayama, S. Hu, C. Chu, Hydrogen peroxide photosynthesis from water and air using a scaled-up 1-m2 flow reactor, Chem Catalysis 5 (2025) 101238. doi:10.1016/j.checat.2024.101238.

[23] M. Osman, I. Qureshi, Review of photovoltaic and concentrated solar technologies including their performance, reliability, efficiency and storage, Results in Engineering 25 (2025). doi:10.1016/j.rineng.2025.104424.

[24] V. Madadi Avargani, S. Zendehboudi, X. Duan, S. Imtiaz, Integrated experimental and multiphysics modeling investigation of a novel photocatalytic reactor for sustainable hydrogen production, Chemical Engineering Journal 521 (2025). doi:10.1016/j.cej.2025.166228.

[25] L. Wang, D. Lei, P. Ren, Y. Lv, N. Luo, Z. Wang, Experimental study on concentrated light photothermal catalytic glycerol for hydrogen production using a novel linear concentrated light flow reactor, Renew. Energy 231 (2024). doi:10.1016/j.renene.2024.120980.

[26] B.C. Ma, H. Lin, Y. Zhu, Z. Zeng, J. Geng, D. Jing, A new Concentrated Photovoltaic Thermal-Hydrogen system with photocatalyst suspension as optical liquid filter, Renew. Energy 194 (2022) 1221–1232. doi:10.1016/j.renene.2022.06.013.

[27] I. Holmes-Gentle, S. Tembhurne, C. Suter, S. Haussener, Kilowatt-scale solar hydrogen production system using a concentrated integrated photoelectrochemical device, Nat. Energy 8 (2023) 586–596. doi:10.1038/s41560-023-01247-2.

[28] D.K. Patel, P.K. Brahmbhatt, H. Panchal, A review on compound parabolic solar concentrator for sustainable development, International Journal of Ambient Energy 39 (2018) 533–546. doi:10.1080/01430750.2017.1318786.

[29] D.I. Paul, Application of compound parabolic concentrators to solar photovoltaic conversion: A comprehensive review, Int. J. Energy Res. 43 (2019) 4003–4050. doi:10.1002/er.4428.

[30] R.V. Parupudi, H. Singh, M. Kolokotroni, J. Tavares, Long term performance analysis of low concentrating photovoltaic (LCPV) systems for building retrofit, Appl. Energy 300 (2021). doi:10.1016/j.apenergy.2021.117412.

[31] V. Bhalla, V. Khullar, R.V. Parupudi, Design and thermal analysis of nanofluid-based compound parabolic concentrator, Renew. Energy 185 (2022) 348–362.

Journal Pre-proof

doi:10.1016/j.renene.2021.12.064.

[32] F. Masood, N.B.M. Nor, P. Nallagownden, I. Elamvazuthi, R. Saidur, M.A. Alam, J. Akhter, M. Yusuf, M. Mehmood, M. Ali, A Review of Recent Developments and Applications of Compound Parabolic Concentrator-Based Hybrid Solar Photovoltaic/Thermal Collectors, Sustainability (Switzerland) 14 (2022). doi:10.3390/su14095529.

[33] D. Jing, H. Liu, X. Zhang, L. Zhao, L. Guo, Photocatalytic hydrogen production under direct solar light in a CPC based solar reactor: Reactor design and preliminary results, Energy Convers. Manag. 50 (2009) 2919–2926. doi:10.1016/j.enconman.2009.07.012.

[34] Q. Wei, Y. Yang, J. Hou, H. Liu, F. Cao, L. Zhao, Direct solar photocatalytic hydrogen generation with CPC photoreactors: System development, Solar Energy 153 (2017) 215–223. doi:10.1016/j.solener.2017.05.064.

[35] Q. Wei, Y. Yang, H. Liu, J. Hou, M. Liu, F. Cao, L. Zhao, Experimental study on direct solar photocatalytic water splitting for hydrogen production using surface uniform concentrators, Int. J. Hydrogen Energy 43 (2018) 13745–13753. doi:10.1016/j.ijhydene.2018.01.135.

[36] Y. Yang, Q. Wei, J. Hou, H. Liu, L. Zhao, Solar concentrator with uniform irradiance for particulate photocatalytic hydrogen production system, Int. J. Hydrogen Energy 41 (2016) 16040–16047. doi:10.1016/j.ijhydene.2016.06.074.

[37] Y. Yang, Y. Zheng, S. Liu, M. Shan, J. Guo, R. Yang, L. Zhao, D. Jing, Deep learning prediction of photocatalytic water splitting for hydrogen production under natural light based on experiments, Energy Convers. Manag. 301 (2024). doi:10.1016/j.enconman.2023.118007.

[38] F. Cao, Q. Wei, H. Liu, N. Lu, L. Zhao, L. Guo, Development of the direct solar photocatalytic water splitting system for hydrogen production in Northwest China: Design and evaluation of photoreactor, Renew. Energy 121 (2018) 153–163. doi:10.1016/j.renene.2018.01.016.

[39] F. Cao, H. Liu, Q. Wei, L. Zhao, L. Guo, Experimental study of direct solar photocatalytic water splitting for hydrogen production under natural circulation conditions, Int. J. Hydrogen Energy 43 (2018) 13727–13737. doi:10.1016/j.ijhydene.2017.12.107.

[40] C. Huang, W. Yao, A. T-Raissi, N. Muradov, Development of efficient photoreactors for solar hydrogen production, Solar Energy 85 (2011) 19–27. doi:10.1016/j.solener.2010.11.004.

[41] Q. Wei, Y. Yang, J. Hou, H. Liu, F. Cao, L. Zhao, Direct solar photocatalytic hydrogen generation with CPC photoreactors: System development, Solar Energy 153 (2017) 215–223. doi:10.1016/j.solener.2017.05.064.

[42] M.J. Uddin, F. Cesano, A.R. Chowdhury, T. Trad, S. Cravanzola, G. Martra, L. Mino, A. Zecchina, D. Scarano, Surface Structure and Phase Composition of TiO2 P25 Particles After Thermal Treatments and HF Etching, Front. Mater. 7 (2020). doi:10.3389/fmats.2020.00192.

[43] J. Krýsa, M. Keppert, J. Jirkovský, V. Štengl, J. Šubrt, The effect of thermal treatment on the properties of TiO2 photocatalyst, Mater. Chem. Phys. 86 (2004) 333–339. doi:10.1016/j.matchemphys.2004.03.021.

[44] N.R.C. Fernandes Machado, V.S. Santana, Influence of thermal treatment on the structure and photocatalytic activity of TiO2 P25, Catal. Today 107–108 (2005) 595–601. doi:10.1016/j.cattod.2005.07.022.
[45] C.S. Gopinath, N. Nalajala, A scalable and thin film approach for solar hydrogen generation: A review on enhanced photocatalytic water splitting, J. Mater. Chem. A Mater. 9 (2021) 1353–1371. doi:10.1039/d0ta09619a.
[46] J. Oberbichler, D.M. Köpfler, M. Wolf, S. Götz, T. Dimopoulos, M.Y.S. Ibrahim, Integrating coating design and reactor engineering for efficient photocatalytic hydrogen evolution in flow systems, Int. J. Hydrogen Energy 235 (2026). doi:10.1016/j.ijhydene.2026.155131.
[47] T.T. Shih, I.H. Hsu, J.F. Wu, C.H. Lin, Y.C. Sun, Development of chip-based photocatalyst-assisted reduction device to couple high performance liquid chromatography and inductively coupled plasma-mass spectrometry for determination of inorganic selenium species, J. Chromatogr. A 1304 (2013) 101–108. doi:10.1016/j.chroma.2013.06.067.

Highlights

- Integrated experimental-computational design framework for optimising solar photocatalytic hydrogen production
- Optimised CPC reflector fitted photocatalytic reactor geometries and orientations for London, Cardiff, Cairo and Chennai
- Hydrogen production rates for London, Cardiff, Cairo and Chennai for five peak solar months
- Annual optical efficiency of solar concentrators
- Experiments to identify peak hydrogen production conditions.

Journal Pre-proof